JACS
JOURNAL OF THE AMERICAN CHEMICAL SOCIETY
pubs.acs.org/JACS
Communication

NMR Signatures and Electronic Structure of Ti Sites in Titanosilicalite-1 from Solid-State $^{47/49}$Ti NMR Spectroscopy

Lukas Lätsch, Christoph J. Kaul, Alexander V. Yakimov, Imke B. Müller, Alia Hassan, Barbara Perrone, Sadig Aghazada, Zachariah J. Berkson, Trees De Baerdemaeker, Andrei-Nicolae Parvulescu, Karsten Seidel, J. Henrique Teles, and Christophe Copéret*

Cite This: *J. Am. Chem. Soc.* 2023, 145, 15018−15023
Read Online
ACCESS | Metrics & More | Article Recommendations | Supporting Information

ABSTRACT: Although titanosilicalite-1 (TS-1) is among the most successful oxidation catalysts used in industry, its active site structure is still debated. Recent efforts have mostly focused on understanding the role of defect sites and extraframework Ti. Here, we report the $^{47/49}$Ti signature of TS-1 and molecular analogues [Ti(OTBOS)$_4$] and [Ti(OTBOS)$_3$(O^{i}Pr)] using novel MAS CryoProbe to enhance the sensitivity. While the dehydrated TS-1 displays chemical shifts similar to those of molecular homologues, confirming the tetrahedral environment of Ti consistent with X-ray absorption spectroscopy, it is associated with a distribution of larger quadrupolar coupling constants, indicating an asymmetric environment. Detailed computational studies on cluster models highlights the high sensitivity of the NMR signatures (chemical shift and quadrupolar coupling constant) to small local structural changes. These calculations show that, while it will be difficult to distinguish mono- vs dinuclear sites, the sensitivity of the $^{47/49}$Ti NMR signature should enable distinguishing the Ti location among specific T site positions.

Titanosilicates belong to an important class of heterogeneous catalysts where Ti is typically incorporated into the crystalline lattice of a zeolite-type framework.[1] The discovery of titanosilicalite-1 (TS-1) *ca.* 40 years ago enabled the development of sustainable processes based on H_2O_2 as a primary oxidant, leaving H_2O as the sole byproduct.[2] Notable industrial examples are the hydroxylation of phenol,[3] the epoxidation of propylene,[4] and the ammoximation of ketones.[5,6] TS-1 has been proposed to contain isolated framework tetrahedral Ti sites, generated by substitution of a small fraction of Si atoms in the zeolite structure.[7] Note that the coordination environment of Ti can be dramatically influenced by the preparation method and the state of the catalysts; such sites include partially hydrolyzed octahedral sites,[8] pentacoordinated sites,[9] tetrahedral titanols,[10] and octahedral defect sites.[11] Recently, paired Ti sites have been evidenced when TS-1 is reacted with H_2O_2.[12]

The coordination environment in titanosilicates was addressed by direct and indirect characterization methods. The latter relies on using probe molecules such as phosphines[13] or pyridine[14] as well as reactants, e.g. H_2O_2,[12] in combination with IR and/or solid-state nuclear magnetic resonance (ssNMR) spectroscopy. Direct approaches have focused on UV/vis, Raman, and X-ray absorption spectroscopy (K and $L_{2,3}$ edge XANES).[11,15] Even though these techniques can provide information about the extent of Ti incorporation into the framework or the ratio of tetrahedral to octahedral Ti sites, they are limited to averaged local structural information and rely mostly on empirical interpretation. In addition, information on preferential Ti siting at different tetrahedral (T) positions can be obtained from neutron powder diffraction (NPD) analysis, but the interpretation is often complicated by the difficulty in distinguishing between Ti sites and silicon vacancies.[16−19]

$^{47/49}$Ti ssNMR spectroscopy could be an alternative direct characterization method to access nonaveraged information on the local coordination geometry of Ti.[20−22] Titanium possesses two NMR-active nuclei, ^{47}Ti (I = 5/2) and ^{49}Ti (I = 7/2), which are both commonly termed as "unreceptive" due to their low natural abundances (7.44% for ^{47}Ti and 5.41% for ^{49}Ti), moderate quadrupole moments ($Q(^{47}\text{Ti})$ = 29.0 fm^2 and $Q(^{49}\text{Ti})$ = 24.0 fm^2), and low gyromagnetic ratios ($\gamma(^{47}\text{Ti}) = -1.5105 \times 10^7$ rad s^{-1} T^{-1}, $\gamma(^{49}\text{Ti}) = -1.51095 \times 10^7$ rad s^{-1} T^{-1}).[23] Due to close gyromagnetic ratios, NMR signals from ^{47}Ti and ^{49}Ti usually overlap, which further complicates analysis.[24] To date, $^{47/49}$Ti ssNMR spectroscopy has been mostly limited to the investigation of bulk materials such as titanium oxides and carbides,[25−27] as well as Ti-USY, a favorable zeotype material with only one framework T site, where signal detection was facilitated by high Ti loading (∼20 wt %).[21] However, analysis of zeolites with industrially relevant Ti loadings (typically 1.5 wt %) and a multitude of available T sites such as TS-1 have previously not been possible. Yet, the characterization of Ti sites in titanocene chlorides demonstrates the sensitivity of $^{47/49}$Ti ssNMR to local structure.[24,28]

The scope of $^{47/49}$Ti ssNMR has been expanded through the development of novel pulse sequences and/or the use of

Received: September 15, 2022
Published: July 7, 2023

dynamic nuclear polarization surface-enhanced NMR spectroscopy (DNP-SENS),[29] which has enabled the detection of Ti surface signals in hydrated TiO_2-supported MoO_3, albeit necessitating a very high concentration of polarizing agent. So far, ssNMR spectroscopy of low-γ quadrupolar nuclei such as $^{47/49}$Ti remains challenging for samples with low Ti loadings (few wt %) and/or containing Ti with large C_Q (e.g., > 15 MHz).

Here, we report the $^{47/49}$Ti ssNMR signatures of a typical titanosilicate-1 catalyst (1.5 wt % Ti) and their relation to the electronic structure of Ti sites obtained from analysis of related solid-state Ti oxides anatase and rutile and molecular compounds—$[Ti(OTBOS)_4]$ (OTBOS = tris(*tert*-butoxy)-siloxy) and $[Ti(OTBOS)_3(O^iPr)]$. The measurements were enabled by the recent development of a low-γ solid-state NMR probe with cryogenic cooling of electronic components (CryoProbe with thermally decoupled sample temperature) for a B_0 field of 18.8 T, which significantly boosts NMR signal sensitivity under both static and magic angle spinning (MAS) conditions.[30] In particular, the use of MAS enables the resolution of ^{47}Ti and ^{49}Ti NMR signals. Comparison of the NMR signatures of Ti in TS-1 and its molecular homologue ($[Ti(OTBOS)_4]$) shows a similar chemical shift, accompanied by a pronounced difference in C_Q that originates from the structure enforced by the zeolite framework. The differences indicate more distorted Ti sites in the zeolite framework compared to molecular siloxide compounds.

To evaluate the sensitivity of the CryoProbe, ssNMR spectra of anatase TiO_2 (60 wt % Ti) were recorded under static (WURST-QCMPG)[31] and MAS (DFS-QCPMG-MAS) conditions.[32,33] The sensitivity per unit time was compared to measurements performed with a low-temperature probe at 14.1 T, available in our laboratory, where the sample rests at *ca.* 100 K (details are provided in the Supporting Information). The CryoProbe sensitivity enhancement factor was estimated to be 10−15, arising from cryogenic cooling of the RF coil and preamplifier electronics (~4×), as well as a larger active sample volume (~3×) owing to longer rotors that the CryoProbe uses.[34] The sensitivity gain from the higher field (18.8 T) is roughly compensated for with low-temperature measurements at 14.1 T (100 K). Additionally, the measurement with the CryoProbe at room temperature favors faster relaxation, which allows a further decrease in the measurement time. Note that the gain from signal narrowing and relaxation is sample dependent. Notably, as anatase shows a reasonably small C_Q (~5 MHz), its ^{47}Ti and ^{49}Ti signals can be resolved under MAS. This enables a more facile interpretation of the spectroscopic signature than under static conditions (Figure 1). For rutile, which is associated with larger C_Q, a line width up to >0.2 MHz can be recorded without the need for multiple offsets and spectrum reconstruction (Figure S2 in the Supporting Information).

Having obtained encouraging preliminary results, we focused on more challenging materials such as TS-1, with low Ti loading (here, 1.5 wt %). Both static and MAS spectra were recorded with good signal-to-noise ratios in reasonable times (see Figure 1, S/N_{static} = 21, t = 3 days and S/N_{MAS} = 65, t = 1 day) for the dehydrated TS-1 sample, which was chosen in order to facilitate NMR measurements due to the presence of highly symmetric tetrahedral Ti sites evidenced by XAS (Figure S4 in the Supporting Information). NMR parameters extracted from the MAS spectra according to the Czjzek model[35] show an isotropic chemical shift (δ_{iso}) of −910 ppm

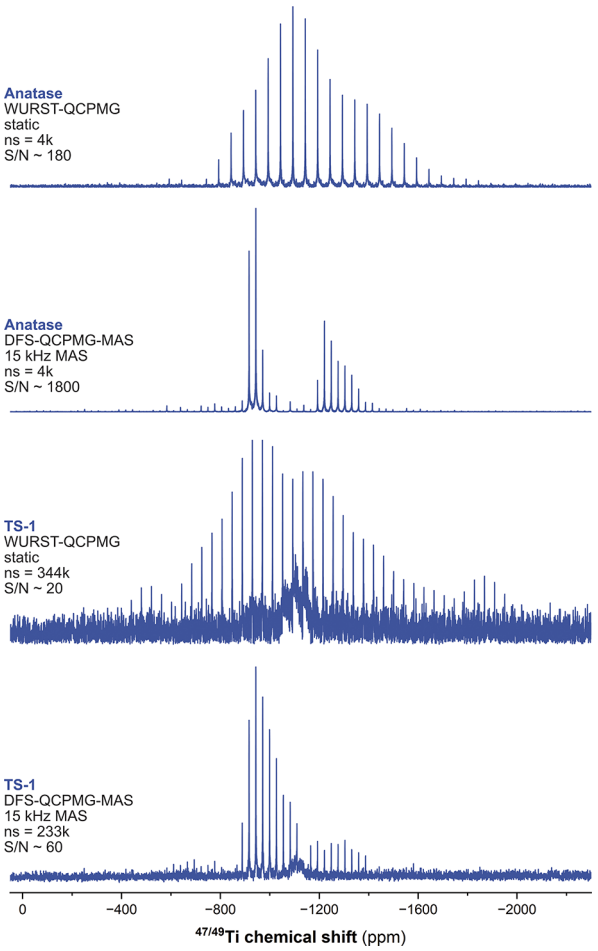

Figure 1. DFS-QCPMG-MAS (15 kHz) and WURST-QCPMG spectra of anatase (top) and TS-1 (bottom) acquired at 298 K and 18.8 T (ns = number of scans, S/N = signal-to-noise ratio), referenced against $SrTiO_3$.

for ^{49}Ti and a distribution of C_Q values with a characteristic value of 7.2 MHz ($C_{Q,max}$), consistent with an all-oxygen distorted-tetrahedral first coordination sphere (*vide infra*). Notably, no signal is observed in the corresponding hydrated TS-1 sample, likely due to the formation of highly distorted Ti sites with very large C_Q values due to hydration: i.e., coordination or reaction with water. This is consistent with pXRD[36] and XAS data, the latter showing a sharp decrease of the pre-edge feature specific of tetrahedral sites upon water adsorption (Figure S4 in the Supporting Information).

Given the response of $^{47/49}$Ti NMR signatures to subtle changes in coordination environment,[24] we next evaluated two tetrahedral molecular complexes. As molecular models for TS-1, $[Ti(OTBOS)_4]$ and $[Ti(OTBOS)_3(O^iPr)]$ were selected, having only oxygens in the first coordination sphere (see the Supporting Information for synthesis and analysis).[37,38] According to a single-crystal X-ray diffraction (XRD) analysis, both molecular models possess near-perfect tetrahedral geometries, as illustrated by their τ_4' values equal to 0.99.[38,39] Homoleptic $[Ti(OTBOS)_4]$ features four crystallographically identical Ti−OSi bonds (1.785 Å), while in the heteroleptic $[Ti(OTBOS)_3(O^iPr)]$, the Ti−OSi bonds are slightly elongated (1.795 Å) and the Ti−O^{i}Pr bond is slightly shortened (1.748 Å). Notably, these compounds, $[Ti(OTBOS)_4]$ and $[Ti(OTBOS)_3(O^iPr)]$, show a pre-edge

https://doi.org/10.1021/jacs.2c09867
J. Am. Chem. Soc. 2023, 145, 15018−15023

feature in Ti K edge XANES spectra typical for tetrahedral complexes, with position and intensity similar to those for TS-1 (Figure S6 in the Supporting Information).[40] In terms of NMR signatures, the chemical shifts appear at δ_{iso} = −910 ppm for the ^{49}Ti sites in TS-1 to be compared with those at −910 and −880 ppm for [Ti(OTBOS)$_4$] and [Ti(OTBOS)$_3$(O^{i}Pr)], respectively. This subtle difference in δ_{iso} between the molecular analogues is accompanied by significantly different C_Q values of 1.8 MHz for [Ti(OTBOS)$_4$] and 4.0 MHz for [Ti(OTBOS)$_3$(O^{i}Pr)], consistent with the asymmetry in the Ti−O bond lengths for the heteroleptic complex. Intriguingly, although TS-1 is expected to have a similar Ti coordination according to the XANES and chemical shift alone, the observed $C_{Q,max}$ of TS-1 (7.2 MHz) is significantly larger than that for both molecular models (Figure 2), pointing to distorted Ti sites.

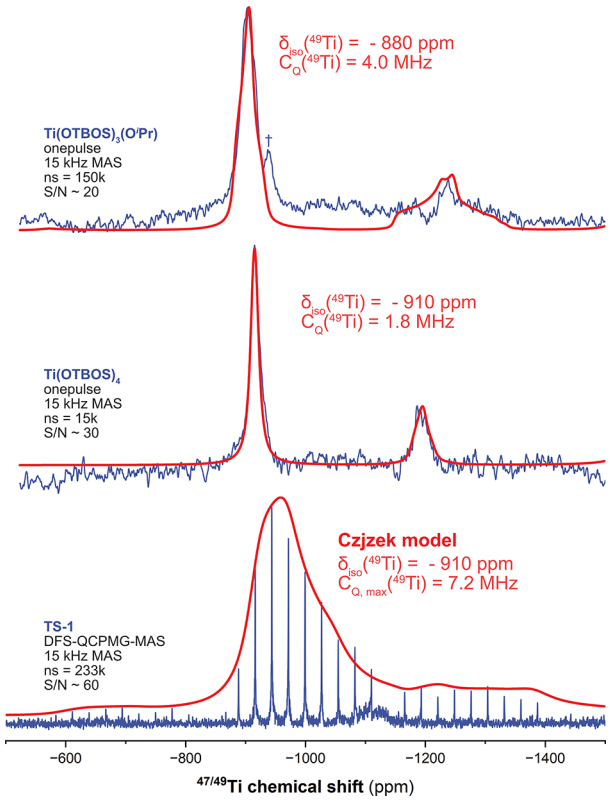

Figure 2. Direct excitation spectra (blue) of [Ti(OTBOS)$_3$(O^{i}Pr)] (top) and [Ti(OTBOS)$_4$] (middle), as well as DFS-QCPMG-MAS spectrum of TS-1 (bottom) all acquired at RT, 18.8 T, and 15 kHz MAS, with corresponding line shape simulations (red), referenced against $SrTiO_3$. † denotes an artifact due to direct excitation and signal processing.

To systematically study the origin of the observed changes within the molecular analogues, we computed the NMR parameters for a series of four-coordinated [Ti(OX)$_4$] models (X = OCH_3, $OSiF_3$, and OCF_3). All compounds show a tetrahedral geometry with different Ti−O−X bond angles, with [Ti(OSiF$_3$)$_4$] displaying more linear bond angles (167°) than [Ti(OCF$_3$)$_4$] (158°) and [Ti(OCH$_3$)$_4$] (153°). Calculated chemical shifts (see the Supporting Information for computational details) for the series are referenced with respect to [Ti(OTBOS)$_4$] ($\Delta\delta_{iso}$ = 0 ppm) and show gradual shielding for more electron withdrawing ligands:[41] [Ti(OCH$_3$)$_4$] ($\Delta\delta_{iso}$ = +31 ppm), [Ti(OSiF$_3$)$_4$] ($\Delta\delta_{iso}$ = −24 ppm), and [Ti(OCF$_3$)$_4$] ($\Delta\delta_{iso}$ = −106 ppm). The agreement between the experimentally observed ($\Delta\delta_{iso}$ = +30 ppm) and the calculated ($\Delta\delta_{iso}$ = +18 ppm (calc.)) chemical shifts for [Ti(OTBOS)$_3$(O^{i}Pr)] in reference to [Ti(OTBOS)$_4$] substantiates the analysis based on model systems.

We next traced back the origin of the chemical shift differences using a natural chemical shift (NCS) analysis that allows the determination of the relative magnetic couplings between occupied and vacant orbitals of appropriate symmetries responsible for paramagnetic deshielding.[42,43] Here, the dominant couplings arise from the σ(Ti−O) and π(Ti−O) frontier orbitals (Figure 3). Higher ligand electro-

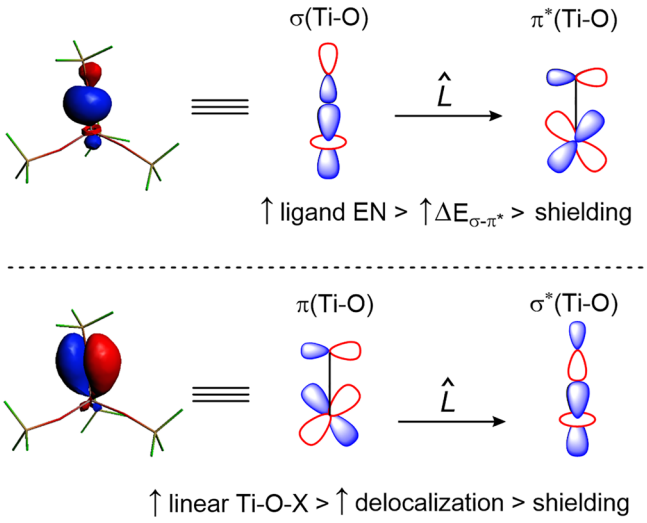

Figure 3. Relevant magnetic couplings that give rise to deshielding in the systems studied herein.

negativity leads to shielding, as the energy gap between the filled σ(Ti−O) and the empty π^*(Ti−O) is raised (*cf.* [Ti(OCH$_3$)$_4$] vs [Ti(OCF$_3$)$_4$]). Shielding can also arise from a more linear Ti−O−X arrangement, as higher electron delocalization may stabilize the π(Ti−O) bonds (*cf.* [Ti(OCH$_3$)$_4$] vs [Ti(OSiF$_3$)$_4$] and [Ti(OTBOS)$_3$(O^{i}Pr)] vs [Ti(OTBOS)$_4$]).

Furthermore, the significantly larger C_Q observed for TS-1 (7.2 MHz) compared with [Ti(OTBOS)$_4$] (1.8 MHz) is also notable. Quadrupolar couplings are particularly sensitive to small changes in the coordination environment, namely coordination number and distortion from ideal geometry, hence providing information on the local surrounding of Ti sites in TS-1, making in principle NMR a complementary technique to neutron diffraction studies.[16,19] For instance, the structurally similar molecular analogues, [Ti(OTBOS)$_4$] and [Ti(OTBOS)$_3$(O^{i}Pr)], show quite different calculated C_Q values of 2.3 and 6.3 MHz, respectively, in line with the experimental values, thus demonstrating the sensitivity of C_Q to small differences in coordination environment, where a simple substitution of OTBOS by O^{i}Pr induces a change in charge distribution, associated with the asymmetry in Ti−O bond lengths.

Expanding on the aforementioned information on the molecular analogues, we further evaluate the sensitivity of chemical shift and the quadrupolar coupling constant (C_Q) for Ti sites constrained within the zeolite framework. Toward this end, we used periodic models where one silicon atom of the

https://doi.org/10.1021/jacs.2c09867
J. Am. Chem. Soc. 2023, 145, 15018−15023

MFI structure is substituted by a Ti atom at various T positions and for which the local geometry around the Ti atom was either fixed or allowed to relax. We also investigated models with monomeric and dimeric Ti sites in view of our recent findings (see the Supporting Information for details).[12] The NMR parameters of all these Ti sites were then calculated by cutting cluster models terminated by fluorine atoms in order to evaluate the effect of T positions, monomeric and dimeric sites, with and without relaxed structures. Overall, the calculated NMR parameters—chemical shifts and C_Q—depend notably on the T site positions and only marginally on having monomeric vs dimeric sites (see Figure S11 in the Supporting Information for further details). Most notable, however, is that the calculated NMR parameters are highly dependent on the underlying periodic model used for the cluster models. While uncertainty of the calculated chemical shift values, obtained from our benchmark calculations, prohibits direct comparison with absolute values observed in experiment, the obtained C_Q values span more than 30 MHz as a function of T site and model. Notably, the values dramatically increase for each T site upon geometry optimization due to increased local distortion. At this stage, $^{47/49}$Ti NMR is in principle sensitive enough to distinguish between specific T sites due to the sensitivity of the NMR parameters, but would require developing more robust NMR calculation methodologies on realistic periodic models, that include effects related to local vs periodic structural parameters, e.g. unit cell expansion upon Ti substitution, dynamics, and defect sites in zeolite structure as well as extraframework Ti sites to name but a few.

In conclusion, we obtained the $^{47/49}$Ti ssNMR signatures of TS-1, despite the low Ti loading (<2 wt %). A comparison to molecular model complexes reveals that dehydrated TS-1 shows a distribution of larger quadrupolar coupling constants, which points toward more distorted Ti sites in the TS-1 structure, despite similar XAS signatures between molecular systems and TS-1. Furthermore, the absence of a $^{47/49}$Ti NMR signal for the hydrated TS-1 shows that Ti sites in the zeolite framework can adapt even more asymmetric local geometries upon adsorption of molecules (e.g., upon exposure to the atmosphere or under reaction conditions). Overall, this study highlights the feasibility of direct characterization of metal sites without a probe molecule and opens the possibility to investigate other industrially relevant titanosilicate catalysts to address the coordination environment and electronic structure of the respective Ti sites. We are currently working on exploring and developing more advanced computational models and protocols to ascribe observed NMR signatures to Ti sites in different T positions of the MFI framework.

■ ASSOCIATED CONTENT

Supporting Information

The Supporting Information is available free of charge at https://pubs.acs.org/doi/10.1021/jacs.2c09867.

Synthesis protocols and corresponding solution NMR, single-crystal XRD structures, solid-state NMR measurement and fitting parameters, Ti K-edge XANES measurement conditions and spectra, powder XRD, DFT calculation protocols for NMR parameters (PDF)

Cartesian coordinates for the calculated structures (ZIP)

Accession Codes

CCDC 2205478 contains the supplementary crystallographic data for this paper. These data can be obtained free of charge via www.ccdc.cam.ac.uk/data_request/cif, or by emailing data_request@ccdc.cam.ac.uk, or by contacting The Cambridge Crystallographic Data Centre, 12 Union Road, Cambridge CB2 1EZ, UK; fax: +44 1223 336033.

■ AUTHOR INFORMATION

Corresponding Author

Christophe Copéret − *ETH Zurich, Department of Chemistry and Applied Biosciences, CH-8093 Zurich, Switzerland; Bruker Switzerland, CH-8117 Fällanden, Switzerland;* orcid.org/0000-0001-9660-3890; Email: ccoperet@ethz.ch

Authors

Lukas Lätsch − *ETH Zurich, Department of Chemistry and Applied Biosciences, CH-8093 Zurich, Switzerland;* orcid.org/0000-0002-0125-6396

Christoph J. Kaul − *ETH Zurich, Department of Chemistry and Applied Biosciences, CH-8093 Zurich, Switzerland*

Alexander V. Yakimov − *ETH Zurich, Department of Chemistry and Applied Biosciences, CH-8093 Zurich, Switzerland;* orcid.org/0000-0002-8624-1002

Imke B. Müller − *BASF SE, 67056 Ludwigshafen am Rhein, Germany*

Alia Hassan − *Bruker Switzerland, CH-8117 Fällanden, Switzerland*

Barbara Perrone − *Bruker Switzerland, CH-8117 Fällanden, Switzerland*

Sadig Aghazada − *ETH Zurich, Department of Chemistry and Applied Biosciences, CH-8093 Zurich, Switzerland;* orcid.org/0000-0002-7568-4481

Zachariah J. Berkson − *ETH Zurich, Department of Chemistry and Applied Biosciences, CH-8093 Zurich, Switzerland;* orcid.org/0000-0002-2157-4172

Trees De Baerdemaeker − *BASF SE, 67056 Ludwigshafen am Rhein, Germany;* orcid.org/0000-0003-4597-0628

Andrei-Nicolae Parvulescu − *BASF SE, 67056 Ludwigshafen am Rhein, Germany*

Karsten Seidel − *BASF SE, 67056 Ludwigshafen am Rhein, Germany*

J. Henrique Teles − *BASF SE, 67056 Ludwigshafen am Rhein, Germany;* orcid.org/0000-0002-7843-5675

Complete contact information is available at: https://pubs.acs.org/10.1021/jacs.2c09867

Notes

The authors declare no competing financial interest.

■ ACKNOWLEDGMENTS

L.L. thanks the Scholarship Fund of the Swiss Chemical Industry (SSCI) and BASF for funding. C.J.K. acknowledges the Swiss National Science Foundation (SNF IZLCZ0_206049). A.V.Y. and Z.J.B. are grateful for SynMatLab for funding. S.A. acknowledges a fellowship from the Swiss National Science Foundation (P5R5PN_202658). We thank Dr. D. Nater for assistance with the XRD measurements. Recording of XRD powder diffractograms by Dirk Paulus and Murat Yavuz (BASF SE, Ludwigshafen) is kindly acknowledged. The Swiss Norwegian beamlines (SNBL, ESRF) are acknowledged for provision of beamtime through

proposal 31-01-143. We thank Dr. W. van Beek and Dr. D. Stoian for their support during XAS experiments.

REFERENCES

(1) Smeets, V.; Gaigneaux, E. M.; Debecker, D. P. Titanosilicate Epoxidation Catalysts: A Review of Challenges and Opportunities. *ChemCatChem.* **2022**, *14* (1), 1−26.
(2) Xu, H.; Wu, P. Recent Progresses in Titanosilicates. *Chin. J. Chem.* **2017**, *35* (6), 836−844.
(3) Romano, U.; Esposito, A.; Maspero, F.; Neri, C.; Clerici, G. M. Selective oxidation with Ti-silicalite. *Chim.Ind.(Milan).* **1990**; p 610−616.
(4) Lin, M.; Xia, C.; Zhu, B.; Li, H.; Shu, X. Green and Efficient Epoxidation of Propylene with Hydrogen Peroxide (HPPO Process) Catalyzed by Hollow TS-1 Zeolite: A 1.0 Kt/a Pilot-Scale Study. *Chem. Eng. J. (Amsterdam, Neth.)* **2016**, *295*, 370−375.
(5) Ge, Q.; Lu, J.; Zhu, M. Research Progress of Titanium Silicalite Molecular Sieve for Cyclohexanone Ammoximation; *Hecheng Xianwei Gongye*: *38*(1), 54−58, **2015**.
(6) Li, M.; Liu, J.; Na, H. Application and Advancements in Synthesis of 2-Butanone Oxime; *Huaxue Gongchengshi*: *20* (7), 42−43, **2006**.
(7) Taramasso, M.; Perego, G.; Notari, B. US4410501A, 1983.
(8) Guo, Q.; Sun, K.; Feng, Z.; Li, G.; Guo, M.; Fan, F.; Li, C. A Thorough Investigation of the Active Titanium Species in TS-1 Zeolite by in Situ UV Resonance Raman Spectroscopy. *Chem. - A Eur. J.* **2012**, *18* (43), 13854−13860.
(9) Zuo, Y.; Liu, M.; Zhang, T.; Hong, L.; Guo, X.; Song, C.; Chen, Y.; Zhu, P.; Jaye, C.; Fischer, D. Role of Pentahedrally Coordinated Titanium in Titanium Silicalite-1 in Propene Epoxidation. *RSC Adv.* **2015**, *5* (23), 17897−17904.
(10) Wang, J.; Chen, Z.; Yu, Y.; Tang, Z.; Shen, K.; Wang, R.; Liu, H.; Huang, X.; Liu, Y. Hollow Core-Shell Structured TS-1@S-1 as an Efficient Catalyst for Alkene Epoxidation. *RSC Adv.* **2019**, *9* (65), 37801−37808.
(11) Signorile, M.; Braglia, L.; Crocellà, V.; Torelli, P.; Groppo, E.; Ricchiardi, G.; Bordiga, S.; Bonino, F. Titanium Defective Sites in TS-1: Structural Insights by Combining Spectroscopy and Simulation. *Angew. Chemie - Int. Ed.* **2020**, *59* (41), 18145−18150.
(12) Gordon, C. P.; Engler, H.; Tragl, A. S.; Plodinec, M.; Lunkenbein, T.; Berkessel, A.; Teles, J. H.; Parvulescu, A. N.; Copéret, C. Efficient Epoxidation over Dinuclear Sites in Titanium Silicalite-1. *Nature* **2020**, *586* (7831), 708−713.
(13) Zhuang, J.; Yan, Z.; Liu, X.; Liu, X.; Han, X.; Bao, X.; Mueller, U. NMR Study on the Acidity of TS-1 Zeolite. *Catal. Lett.* **2002**, *83* (1−2), 87−91.
(14) Gunther, W. R.; Michaelis, V. K.; Griffin, R. G.; Roman-Leshkov, Y. Interrogating the Lewis Acidity of Metal Sites in Beta Zeolites with ^{15}N Pyridine Adsorption Coupled with MAS NMR Spectroscopy. *J. Phys. Chem. C* **2016**, *120* (50), 28533−28544.
(15) Spanjers, C. S.; Guillo, P.; Tilley, T. D.; Janik, M. J.; Rioux, R. M. Identification of Second Shell Coordination in Transition Metal Species Using Theoretical XANES: Example of Ti-O-(C, Si, Ge) Complexes. *J. Phys. Chem. A* **2017**, *121* (1), 162−167.
(16) Henry, P. F.; Weller, M. T.; Wilson, C. C. Structural Investigation of TS-1: Determination of the True Nonrandom Titanium Framework Substitution and Silicon Vacancy Distribution from Powder Neutron Diffraction Studies Using Isotopes. *J. Phys. Chem. B* **2001**, *105* (31), 7452−7458.
(17) Dong, J.; Zhu, H.; Xiang, Y.; Wang, Y.; An, P.; Gong, Y.; Liang, Y.; Qiu, L.; Zheng, A.; Peng, X.; Lin, M.; Xu, G.; Guo, Z.; Chen, D. Toward a Unified Identification of Ti Location in the MFI Framework of High-Ti-Loaded TS-1: Combined EXAFS, XANES, and DFT Study. *J. Phys. Chem. C* **2016**, *120* (36), 20114−20124.
(18) Hijar, C. A.; Jacubinas, R. M.; Eckert, J.; Henson, N. J.; Hay, P. J.; Ott, K. C. The Siting of Ti in TS-1 Is Non-Random. Powder Neutron Diffraction Studies and Theoretical Calculations of TS-1 and FeS-1. *J. Phys. Chem. B* **2000**, *104* (51), 12157−12164.
(19) Lamberti, C.; Bordiga, S.; Zecchina, A.; Artioli, G.; Marra, G.; Spanò, G. Ti Location in the MFI Framework of Ti-Silicalite-1: A Neutron Powder Diffraction Study. *J. Am. Chem. Soc.* **2001**, *123* (10), 2204−2212.
(20) Lucier, B. E. G.; Huang, Y. *Reviewing 47/49 Solid-State NMR Spectroscopy: From Alloys and Simple Compounds to Catalysts and Porous Materials*, 1st ed.; Elsevier: 2016; Vol. *88*.
(21) Ganapathy, S.; Gore, K. U.; Kumar, R.; Amoureux, J. P. Multinuclear (^{27}Al, ^{29}Si, ^{47,49}Ti) Solid-State NMR of Titanium Substituted Zeolite USY. *Solid State Nucl. Magn. Reson.* **2003**, *24*, 184−195.
(22) Lopez, A.; Tuilier, M. H.; Guth, J. L.; Delmotte, L.; Popa, J. M. Titanium in MFI-Type Zeolites: A Characterization by XANES, EXAFS, IR, and ^{74,49}Ti and ^{17}O MAS NMR Spectroscopy and H2O Adsorption. *J. Solid State Chem.* **1993**, *102*, 480−491.
(23) Harris, R. K.; Becker, E. D.; Cabral de Menezes, S. M.; Goodfellow, R.; Granger, P. NMR Nomenclature. Nuclear Spin Properties and Conventions for Chemical Shifts (IUPAC Recommendations 2001). *Pure Appl. Chem.* **2001**, *73* (11), 1795−1818.
(24) Rossini, A. J.; Hung, I.; Schurko, R. W. Solid-State $^{47/49}$Ti NMR of Titanocene Chlorides. *J. Phys. Chem. Lett.* **2010**, *1* (20), 2989−2998.
(25) Stephens, K. J.; Zichittella, G.; Saadun, A. J.; Buchele, S.; Puertolas, B.; Verel, R.; Krumeich, F.; Willinger, M.-G.; Perez-Ramirez, J. Transformation of Titanium Carbide into Mesoporous Titania for Catalysed HBr Oxidation. *Catal. Sci. Technol.* **2020**, *10* (12), 4072−4083.
(26) Gervais, C.; Smith, M. E.; Pottier, A.; Jolivet, J. P.; Babonneau, F. Solid-State ^{47,49}Ti MNR Determination of the Phase Distribution of Titania Nanoparticles. *Chem. Mater.* **2001**, *13* (2), 462−467.
(27) Larsen, F. H.; Farnan, I.; Lipton, A. S. Separation of ^{47}Ti and ^{49}Ti Solid-State NMR Lineshapes by Static QCPMG Experiments at Multiple Fields. *J. Magn. Reson.* **2006**, *178* (2), 228−236.
(28) For example, the spectroscopic signatures of $CpTiCl_3$ and Cp^*TiCl_3 showed an increased chemical shift anisotropy (CSA) by >500 ppm upon replacing the protons of the cyclopentadienyl (Cp) ligand by methyl groups (Cp*). However, measurement of these molecular complexes was only possible because of their pseudotetrahedral geometry, yielding relatively small quadrupolar coupling constants (C_Q < 6 MHz).
(29) Nagashima, H.; Trebosc, J.; Kon, Y.; Sato, K.; Lafon, O.; Amoureux, J.-P. Observation of Low-γ Quadrupolar Nuclei by Surface-Enhanced NMR Spectroscopy. *J. Am. Chem. Soc.* **2020**, *142* (24), 10659−10672.
(30) Hassan, A.; Quinn, C. M.; Struppe, J.; Sergeyev, I. V.; Zhang, C.; Guo, C.; Runge, B.; Theint, T.; Dao, H. H.; Jaroniec, C. P.; Berbon, M.; Lends, A.; Habenstein, B.; Loquet, A.; Kuemmerle, R.; Perrone, B.; Gronenborn, A. M.; Polenova, T. Sensitivity Boosts by the CPMAS CryoProbe for Challenging Biological Assemblies. *J. Magn. Reson.* **2020**, *311*, 106680.
(31) Schurko, R. W. Ultra-Wideline Solid-State NMR Spectroscopy. *Acc. Chem. Res.* **2013**, *46* (9), 1985−1995.
(32) Iuga, D.; Schäfer, H.; Verhagen, R.; Kentgens, A. P. M. Population and Coherence Transfer Induced by Double Frequency Sweeps in Half-Integer Quadrupolar Spin Systems. *J. Magn. Reson.* **2000**, *147* (2), 192−209.
(33) Larsen, F. H.; Jakobsen, H. J.; Ellis, P. D.; Nielsen, N. C. QCPMG-MAS NMR of Half-Integer Quadrupolar Nuclei. *J. Magn. Reson.* **1998**, *131* (1), 144−147.
(34) Styles, P.; Soffe, N. F.; Scott, C. A.; Cragg, D. A.; Row, F.; White, D. J.; White, P. C. J. A High-Resolution NMR Probe in Which the Coil and Preamplifier Are Cooled with Liquid Helium. *J. Magn. Reson.* **2011**, *213* (2), 347−354.
(35) d'Espinose de Lacaillerie, J. B.; Fretigny, C.; Massiot, D. MAS NMR Spectra of Quadrupolar Nuclei in Disordered Solids: The Czjzek Model. *J. Magn. Reson.* **2008**, *192* (2), 244−251.
(36) Note that powder X-ray diffraction of the hydrated and dehydrated samples (for details see Figure S5 in the Supporting

https://doi.org/10.1021/jacs.2c09867
J. Am. Chem. Soc. 2023, 145, 15018−15023

Information) show no sizable difference, indicating that water coordination to Ti is the primary reason for the observed signal loss.
(37) Coles, M. P.; Lugmair, C. G.; Terry, K. W.; Tilley, T. D. Titania-Silica Materials from the Molecular Precursor Ti[OSi-(O^{t}Bu)$_3$]$_4$: Selective Epoxidation Catalysts. *Chem. Mater.* **2000**, *12* (1), 122−131.
(38) Noh, G.; Lam, E.; Alfke, J. L.; Larmier, K.; Searles, K.; Wolf, P.; Copéret, C. Selective Hydrogenation of CO_2 to CH_3OH on Supported Cu Nanoparticles Promoted by Isolated Ti^{IV} Surface Sites on SiO_2. *ChemSusChem* **2019**, *12* (5), 968−972.
(39) Okuniewski, A.; Rosiak, D.; Chojnacki, J.; Becker, B. Coordination Polymers and Molecular Structures among Complexes of Mercury(II) Halides with Selected 1-Benzoylthioureas. *Polyhedron* **2015**, *90*, 47−57.
(40) Because of their very small C_Q values CPMG acquisition could not be applied without signal truncation and due to the low Ti wt % contents as the result of using the large siloxide ligands (Ti(OTBOS)$_4$ 4.4 wt % Ti and Ti(OTBOS)$_3$(OiPr) 5.3 wt % Ti) only MAS spectra were recorded.
(41) Feige, F.; Malaspina, L. A.; Rychagova, E.; Ketkov, S.; Grabowsky, S.; Hupf, E.; Beckmann, J. Perfluorinated Trialkoxysilanol with Dramatically Increased Brønsted Acidity. *Chem. - A Eur. J.* **2021**, *27* (64), 15898−15902.
(42) Gordon, C. P.; Lätsch, L.; Copéret, C. Nuclear Magnetic Resonance: A Spectroscopic Probe to Understand the Electronic Structure and Reactivity of Molecules and Materials. *J. Phys. Chem. Lett.* **2021**, *12* (8), 2072−2085.
(43) Ramsey, N. F. Magnetic Shielding of Nuclei in Molecules. *Phys. Rev.* **1950**, *78* (6), 699−703.

https://doi.org/10.1021/jacs.2c09867
J. Am. Chem. Soc. 2023, 145, 15018−15023